Available online at www.sciencedirect.com

ScienceDirect

Energy Procedia 142 (2017) 337–342

Energy Procedia

www.elsevier.com/locate/procedia

9th International Conference on Applied Energy, ICAE2017, 21-24 August 2017, Cardiff, UK

Impact of cross-sectional area ratio on time-averaged pressure drop induced by jet pump for thermoacoustic engine

Ye Feng[a], Ke Tang[a,b,*], Tao Jin[a,b], Kaihao Zhang[c]

[a]*Institute of Refrigeration and Cryogenics, Zhejiang University, Hangzhou 310027, China*

[b]*Key Laboratory of Refrigeration and Cryogenic Technology of Zhejiang Province, Hangzhou 310027, China*

[c]*Department of Mechanical Science and Engineering, University of Illinois, Urbana, IL 61801, USA*

Abstract

Gedeon streaming, a time-averaged mass flow circulating throughout the loop configuration in the oscillating flow, can considerably deteriorate the thermal efficiency of traveling-wave thermoacoustic engine. Jet pump is characterized by a tapered channel with different inlet and outlet areas. It can produce a time-averaged pressure drop to suppress Gedeon streaming. In this study, the suppression mechanism of the jet pump in oscillatory flow is investigated, and the emphasis is put on the effect of cross-sectional area ratio on the performance of jet pumps with different taper angles. An experimental apparatus has been built to measure the time-averaged pressure induced by the jet pump. When the taper angle ranges from 3° to 9°, the time-averaged pressure drop and working efficiency can be improved by increasing cross-sectional area ratio, and the change of taper angle has little effect on the performance of jet pumps. However, as the taper angle increases beyond 9°, the performance of jet pump with a large cross-sectional area ratio degrades considerably. In addition, the time-averaged pressure drops induced by the jet pumps with different cross-sectional area ratios are similar, and the taper angle becomes more dominant for jet pump's performance.

Peer-review under responsibility of the scientific committee of the 9th International Conference on Applied Energy.

Keywords: thermoacoustic engine; jet pump; acoustic streaming; oscillatory flow; time-averaged pressure drop

1. Introduction

The high demand of global energy consumption and the everlasting shortage in supply have imposed us with the challenge to improve the usability of low-grade thermal energy. A thermoacoustic engine based on thermoacoustic

* Corresponding author: Ke Tang. Tel.: +86-571-87953233; fax: +86-571-87953233.
E-mail address: ktang@zju.edu.cn

1876-6102
Peer-review under responsibility of the scientific committee of the 9th International Conference on Applied Energy.
10.1016/j.egypro.2017.12.053

effect is an attractive solution due to its high reliability and longevity as it has no moving parts. It is also environmentally friendly using natural working fluids, such as helium, nitrogen or carbon dioxide. There have been extensive research and development effort on thermoacoustic engine applications in electrical power generation [1], refrigeration [2], and water pumping [3].

Due to the perfect thermal contact between working fluid and solid boundary in the regenerator, a traveling-wave thermoacoustic engine is theoretically more efficient than a standing-wave one [4], thus has more development prospect [5]. However, a traveling-wave thermoacoustic engine usually has a loop configuration, which may cause an acoustic streaming named as Gedeon streaming [6]. The Gedeon streaming is a time-averaged mass flow superimposed on an oscillatory flow, circulating throughout the looped configuration, and it can cause heat loss and severely reduces the efficiency of thermoacoustic engines [7,8].

A "jet pump", proposed by Backhaus and Swift [5], has been used in thermoacoustic engines to suppress the Gedeon streaming. The jet pump is characterized by a tapered hole with different inlet and outlet areas, which can induce a time-averaged pressure drop in oscillatory flow, because the pressure drop through the jet pump is asymmetric between the forward and the backward flow. Such a time-averaged pressure drop can suppress the Gedeon streaming. So far, the time-averaged pressure drop induced by a jet pump is usually calculated by the formula proposed by Backhaus and Swift [5,9]. This is based on Iguchi's hypothesis [10] that the oscillating fluid with large amplitude has no memory on the previous flow at any point, and the flow at each time can be seen as a quasi-static flow. However, the applicability of the Iguchi's hypothesis on a jet pump is still controversial [11,12].

In order to study the resistance characteristics of the jet pump in oscillatory flow, an experimental apparatus has been set up to analyze the time-averaged pressure drop induced by the jet pump. The emphasis is put on the effect of cross-sectional area ratio on the performance of jet pumps with different taper angles.

2. Experimental apparatus and data reduction

2.1. Experimental apparatus

Fig. 1 is the schematic of experimental apparatus used to investigate jet pump's performance. The experimental apparatus consists of a linear compressor, a tested jet pump, a particle packing chamber and a reservoir. The tested jet pump is a stainless steel cylinder with a tapered hole, as shown in Fig. 2. The main dimensions are tabulated in Table 1. For all samples, the ratio of rounding radius to diameter of the small opening r/d_s is 0.3. The cross-sectional area ratio a_b/a_s is defined as the area ratio of the big opening a_b to the small opening a_s.

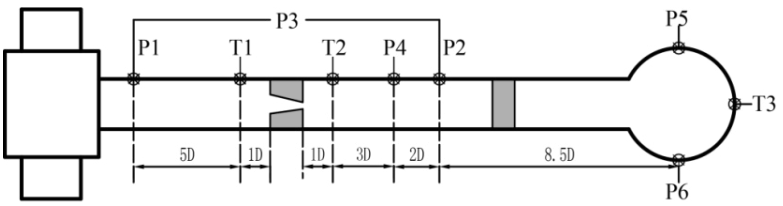

Fig. 1. Schematic of the experimental apparatus

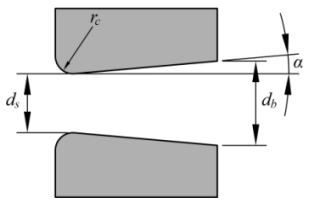

Fig. 2. Schematic of the jet pump

Table 1. Main dimensions of the jet pump

No.	α (°)	a_b/a_s	d_s (mm)	d_b (mm)	L_{JP} (mm)	No.	α (°)	a_b/a_s	d_s (mm)	d_b (mm)	L_{JP} (mm)
1	3	2.04	7	10	30.8	9	9	1.78	6	8	8.3
2	5	2.04	7	10	19.3	10	12	1.78	6	8	6.7
3	7	2.04	7	10	14.4	11	3	1.49	9	11	21.8
4	9	2.04	7	10	11.7	12	5	1.49	9	11	14.3
5	12	2.04	7	10	9.4	13	7	1.49	9	11	11
6	3	1.78	6	8	20.4	14	9	1.49	9	11	9.2
7	5	1.78	6	8	13.3	15	12	1.49	9	11	7.7
8	7	1.78	6	8	10.1						

A resistance-and-compliance (RC) load, which is usually used for measuring the acoustic power output of thermoacoustic engines [5], is adopted to characterize the velocity amplitude through the jet pump. The RC load often takes the form of a needle valve combined with a reservoir. The opening of the needle valve is very small, which may affect the flow field inside the pipe substantially. Here, the particle packing instead of the needle valve is used to provide resistance in our experimental apparatus. The volume of reservoir V_{res} is 1 liter. Nitrogen gas, at a pressure of 3 MPa, is used as the working fluid in the experiment, and the frequency of the oscillatory flow is 60 Hz.

Six pressure sensors and three thermometers are arranged in the system as shown in Fig. 2. The pressure sensors P1 and P2 are located at a same distance of 6D (the diameter of the pipe D is 28 mm) on each side of the jet pump to measure the dynamic pressure, with an accuracy of 3.447 kPa. The pressure drop of the working gas is measured by a two-way differential pressure sensors P3, with the range of −200 to 200 kPa and the accuracy of 0.2% FS. The pressure sensors P4 and P5 are used to measure the mean pressure in the pipe and the reservoir, with the range of 0−5 MPa and the accuracy of 0.2% FS. Since the pressure amplitude in the reservoir is much smaller than that in the pipe, the pressure sensor P6, with an accuracy of 0.57 kPa, is used to measure the dynamic pressure in the reservoir. The temperatures of the working gas at each end of the jet pump, as well as that in the reservoir, are measured by three sheathed PT100 platinum resistance thermometers (i.e., T1, T2 and T3), with accuracies of ±0.1 °C.

2.2. Data reduction

The time-averaged pressure drop and the acoustic power loss can be rewritten as

$$\Delta p_{\mathrm{a}} = \frac{1}{8}\rho u_1^{\,2}\left(k_+ - k_-\right) \tag{1}$$

$$\Delta E = \frac{a_{\mathrm{s}}}{3\pi}\rho u_1^{\,3}\left(k_+ + k_-\right) \tag{2}$$

where ρ is the mean density of working fluid, the k_+ represents the resistance coefficient of forward fluid flow, i.e., the flow in the converging direction, while the k_- means the resistance coefficient of backward fluid flow, i.e., the flow in the diverging direction.

According to Eqs. (1) and (2), k_+ and k_- can be calculated by

$$k_+ = \frac{3\pi\Delta E + 8\Delta p_{\mathrm{a}} a_{\mathrm{s}} u_1}{2\rho u_1^{\,3} a_{\mathrm{s}}} \tag{3}$$

$$k_- = \frac{3\pi\Delta E - 8\Delta p_{\mathrm{a}} a_{\mathrm{s}} u_1}{2\rho u_1^{\,3} a_{\mathrm{s}}} \tag{4}$$

In order to evaluate the performance of a jet pump, three parameters, i.e., the coefficient of time-averaged resistance k_{a}, the coefficient of overall resistance k_{total}, and the coefficient of effectiveness ε, were proposed in our former work to characterize the ability of the jet pump inducing time-averaged pressure drop [13]. The definitions are as follows

$$k_{\mathrm{a}} = \int_0^T \Delta p \mathrm{d}t \Big/ \int_0^T \frac{\rho u^2}{2}\mathrm{d}t = \frac{k_+ - k_-}{2} \tag{5}$$

$$k_{\mathrm{total}} = \int_0^T \left|\Delta p\right| \mathrm{d}t \Big/ \int_0^T \frac{\rho u^2}{2}\mathrm{d}t = \frac{k_+ + k_-}{2} \tag{6}$$

$$\varepsilon = \left| \frac{\Delta p_a}{\Delta E} \right| \tag{7}$$

The coefficient of time-averaged resistance k_a corresponds to the time-averaged pressure drop Δp_a, whereas the coefficient of overall resistance k_{total} corresponds to the total pressure loss Δp_{total}. The coefficient of effectiveness ε denotes the time-averaged pressure drop obtained from unit fluid flow power consumption. In the light of these, a larger k_a means that a jet pump has the higher potential to produce the time-averaged pressure drop. A larger k_{total}, implying the larger overall pressure loss, is not expected. A jet pump with a higher ε can produce a larger time-averaged pressure drop with a given flow power consumption, i.e., a higher working efficiency. The coefficient of effectiveness ε can be calculated by Eq. (7). Substituting Eqs. (3) and (4) into Eqs. (5) and (6) gives

$$k_a = \frac{4\Delta p_a}{\rho u_1^{\,2}} \tag{8}$$

$$k_{total} = \frac{3\pi \Delta E}{2 a_s \rho u_1^{\,3}} \tag{9}$$

Based on the analogy of acoustics and electrics [5], u_1 can be calculated by

$$u_1 = i\omega\rho_{res} \frac{V_{res} p_{1,res} / p_{m,res} + V_2 p_{1,2} / p_{m,pi}}{\gamma \rho_{jp} a_s} \tag{10}$$

where ω is the angular frequency, $U_{1,jp}$ is the volumetric velocity amplitude through the jet pump, C_{res} and C_2 denote acoustic compliances of the reservoir and the pipe between the reservoir and the jet pump, respectively. $p_{1,res}$ and $p_{1,2}$ are the pressure amplitudes in the reservoir and in the pipe behind the jet pump, measured by P6 and P2, respectively. V_2 is the volume of the pipe between the reservoir and jet pump. $p_{m,res}$ and $p_{m,pi}$ are the mean operating pressures in the reservoir and in the pipe, measured by P5 and P4, respectively. γ is the specific heat capacity ratio of the working fluid. ρ_{res} and ρ_{jp} are the densities of fluid in the reservoir and in the jet pump, respectively.

The time-averaged pressure drop Δp_a can be measured by P3. The acoustic power loss ΔE can be calculated by

$$\Delta E = \frac{1}{2}\mathrm{Re}\left(p_{1.1}\tilde{U}_{1,1}\right) - \frac{1}{2}\mathrm{Re}\left(p_{1.2}\tilde{U}_{1,2}\right) \tag{11}$$

where $p_{1,1}$ is the pressure amplitude in the pipe before the jet pump measured by P1. $U_{1,1}$ and $U_{1,2}$ are the volumetric velocity amplitudes on each side of the jet pump, respectively. Diacritical mark ~ stands for complex conjugate. The volumetric velocity amplitudes on each side of the jet pump $U_{1,1}$ and $U_{1,2}$ can be calculated by

$$U_{1,1} = \frac{i\omega V_{res} p_{1,res} \rho_{res}}{\gamma \rho_{jp} p_{m,res}} + i\omega\rho_{res} \frac{V_2 p_{1,2} - V_1 p_{1,1}}{\gamma \rho_{jp} p_{m,pi}} \tag{12}$$

$$U_{1,2} = \frac{i\omega V_{res} \rho_{res} p_{1,res}}{\gamma \rho_{jp} p_{m,res}} - \frac{i\omega\rho_{res} V_3 p_{1,2}}{\gamma \rho_{jp} p_{m,pi}} \tag{13}$$

where C_1 and V_1 are the acoustic compliance and the volume of connecting pipe between P1 and jet pump, respectively. C_3 and V_3 denote the acoustic compliance and the volume of connecting pipe between P2 and reservoir, respectively.

For oscillatory flow, Reynolds number can be defined as $Re=u_1\delta_v\rho/\mu$ [14], where δ_v is the viscous penetration depth, μ is viscosity of the working fluid. Based on the study of Ohmi and Iguchi, the oscillatory flow transforms to turbulence when Re is larger than the critical value $Re_c=305(d/\delta_v)^{1/7}$ [15]. In our experiment, Re is 4×10^3, which is beyond to Re_c, indicating that the flow is in the turbulent region.

3. Experimental results and discussion

The variations of k_+ and k_- with cross-sectional area ratio a_b/a_s for different taper angle α are shown in Fig. 3. For the forward flow, k_+ has a little decrease with a rise in a_b/a_s, as shown Fig. 3(a). In addition, for a given a_b/a_s, the variation of α has little effect on k_+. For the backward flow, the effect of a_b/a_s on k_- is related to α. When α ranges from 3° to 9°, k_- decreases visibly with a_b/a_s, since the local resistance losses through the inlet and outlet openings in the backward flow can be reduced by increasing a_b/a_s. For the jet pumps with α of 12°, k_- changes slightly with a_b/a_s. For the backward flow, i.e., the flow in the diverging direction, the flow may separate from the wall as α becomes larger [13], resulting in the big opening area of jet pump is larger than the actual flowing area, which eventually causes the increase in the expansion loss, and the increase in k_-. For the case with a_b/a_s=1.49, k_- of the jet pump with α of 12° is closed to that with α in the range of 3° to 9°, indicating that there is no flow separation. However, for a larger a_b/a_s, k_- increases visibly for the jet pump with α of 12°, implying the flow separates from the wall, and there is a difference between the actual flowing area and the cross-sectional area of channel. Moreover, the increase of a_b/a_s has little effect on k_-, and α becomes more dominant.

Fig. 4 presents the functions of k_a, k_{total} and ε with a_b/a_s for different α. When α ranges from 3° to 9°, k_a and ε increase, and k_{total} decreases with a rise in a_b/a_s, which means the time-averaged pressure drop and the working efficiency can be improved by increasing a_b/a_s, and the change of α has little effect on the performance. However, as α increases to 12°, for the jet pump with a larger a_b/a_s, the time-averaged pressure drop and the working efficiency decrease, and the total pressure loss increases, indicated by the decreases of k_a and ε, and the increase of k_{total}. And

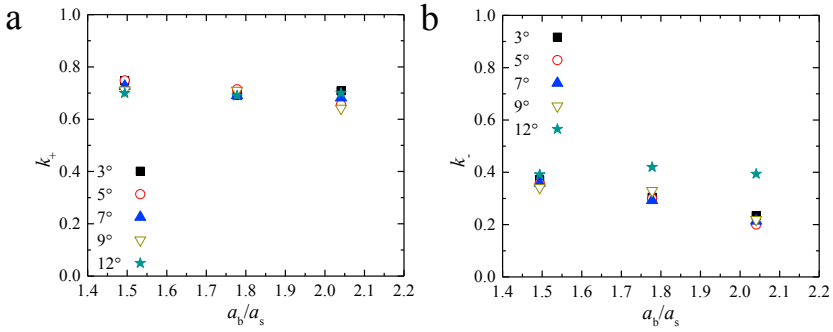

Fig. 3. Variations of coefficients of resistance (a) k_+ and (b) k_- with a_b/a_s for different α.

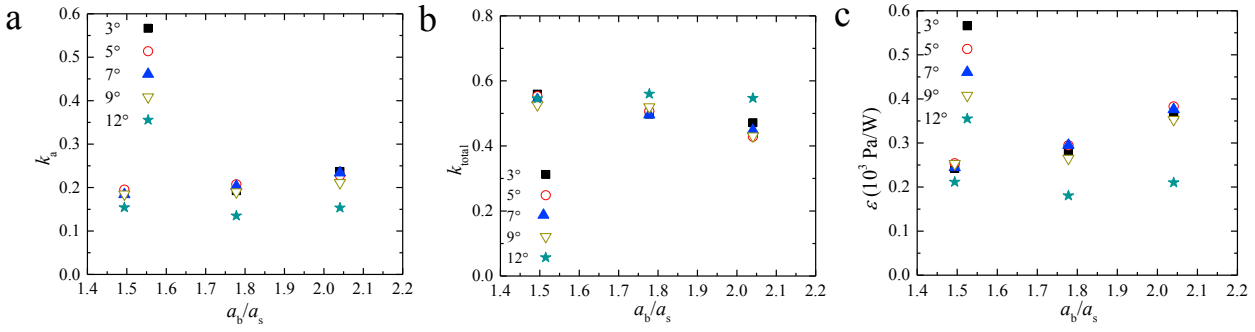

Fig. 4. Variations of (a) coefficient of time-averaged resistance k_a, (b) coefficient of overall resistance k_{total} and (c) coefficient of effectiveness ε with a_b/a_s for different α.

the deteriorate shows a rising trend with the increase of a_b/a_s, which finally results in the jet pumps with different a_b/a_s at α=12° have similar performance. Therefore, during the jet pump design, a_b/a_s should be larger with α in the range of 3° to 9°, which is benefit to improve the jet pump's performance.

4. Conclusion

In order to study the resistance characteristics of the jet pump in oscillating flow, an experimental apparatus has been set up to analyze the time-averaged pressure drop and the working efficiency of the jet pump, and the effect of cross-sectional area ratio a_b/a_s on the performance of jet pumps with different taper angle α has been probed. The experimental results show that when α ranges from 3° to 9°, the time-averaged pressure drop and the working efficiency increase, and the total pressure loss decreases with a rise in a_b/a_s, indicated by the increases of k_a and ε, and the decrease of k_{total}. Moreover, the change of α has little effect on the jet pump's performance. However, as α increases beyond 9°, for the jet pump with a larger a_b/a_s, the performance of jet pump degrades considerably. This can be attributed to the flow separation from the wall in the diverging direction as α becomes larger, which lowers the effect of a_b/a_s on the performance of jet pump. In addition, the time-averaged pressure drops induced by the jet pumps with different cross-sectional area ratios at taper angle of 12° are similar, and the taper angle becomes more dominant for jet pump's performance.

Acknowledgements

This work is financially supported by the National Natural Science Foundation of China (Grant Nos. 51376158 and 51576170) and the National Key Research and Development Program (Grant No. 2016YFB0901403).

References

[1] Bi TJ, Wu ZH, Zhang LM, Yu GY, Luo EC, Dai W. Development of a 5 kW traveling-wave thermoacoustic electric generator. Appl Energy 2017; 185: 1355-61.
[2] Hasegawa S, Yamaguchi T, Oshinoya Y. A thermoacoustic refrigerator driven by a low temperature-differential, high-efficiency multistage thermoacoustic engine. Appl Therm Eng 2013; 58(1-2): 394-9.
[3] Oyewunmi OA, Kirmse CJW, Haslam AJ, Müller EA, Markides CN. Working-fluid selection and performance investigation of a two-phase single-reciprocating-piston heat-conversion engine. Appl Energy 2017; 186: 376-95.
[4] Ceperley PH. A pistonless Stirling engine—the traveling wave heat engine. J Acoust Soc Am 1979; 66(5): 1508-13.
[5] Backhaus S, Swift GW. A thermoacoustic-Stirling heat engine: Detailed study. J Acoust Soc Am 2000; 107(6): 3148-66.
[6] Gedeon D. DC gas flows in Stirling and pulse tube cryocoolers. In: Ross Jr. RG editors. Cryocoolers 9. New York: Plenum Press; 1997. p. 385-92.
[7] Biwa T, Tashiro Y, Ishigaki M, Ueda Y, Yazaki T. Measurements of acoustic streaming in a looped-tube thermoacoustic engine with a jet pump. J Appl Phys 2007; 101(6): 064914.
[8] Tang K, Feng Y, Jin T, Jin S H, Li M, Yang R. Effect of Gedeon streaming on thermal efficiency of a travelling-wave thermoacoustic engine. Appl Therm Eng 2017; 115: 1089-100.
[9] Yang P, Liu YW, Zhong GY. Prediction and parametric analysis of acoustic streaming in a thermoacoustic Stirling heat engine with a jet pump using response surface methodology. Appl Therm Eng 2016; 103: 1004-13.
[10] Iguchi M, Ohmi M, and Meagawa K. Analysis of free oscillatory flow in a U-shaped tube. Bull JSME 1982; 25: 1398-405.
[11] Petculescu A, Wilen LA, Oscillatory flow in jet pumps: Nonlinear effects and minor losses. J Acoust Soc Am 2003; 113(3): 1282-92.
[12] Oosterhuis JP, Bühler S, van der Meer TH, Wilcox D. A numerical investigation on the vortex formation and flow separation of the oscillatory flow in jet pumps. J Acoust Soc Am 2015; 137(4):1722.
[13] Tang K, Feng Y, Jin SH, Jin T, Li M. Performance comparison of jet pumps with rectangular and circular tapered channels for a loop-structured traveling-wave thermoacoustic engine. Appl Energy 2015; 148: 305-13.
[14] Smith BL, Swift GW. Power dissipation and time-averaged pressure in oscillatory flow through a sudden area change. J Acoust Soc Am 2003; 113(5): 2455-63.
[15] Ohmi M, Iguchi M. Critical Reynolds Number in an Oscillating Pipe Flow. Transactions of the Japan Society of Mechanical Engineers B 1982; 25(200): 165-72.